Available online at www.sciencedirect.com
SCIENCE DIRECT®
Polymer 44 (2003) 4491–4499
polymer
www.elsevier.com/locate/polymer

Polyimide/POSS nanocomposites: interfacial interaction, thermal properties and mechanical properties

Jun-chao Huang[a], Chao-bin He[a,*], Yang Xiao[a], Khine Yi Mya[a], Jie Dai[b], Yeen Ping Siow[b]

[a]*Institute of Materials Research and Engineering (IMRE), MBMC, 3 Research Link, Singapore, Singapore 117602*
[b]*DSO National Lab, 20 Science Park Drive, Singapore, Singapore 118230*

Received 19 January 2003; received in revised form 20 May 2003; accepted 27 May 2003

Abstract

A series of functional polyhedral oligomer silsesquioxnae (POSS)/polyimide (PI) nanocomposites were prepared using a two-step approach, first, the octa(aminophenyl)silsesquioxane (OAPS)/NMP solution was mixed with polyamic acid (PAA) solution prepared by reacting 4,4′-diaminodiphenylmethane and 3,3′,4,4′-benzophenonetetracarboxylic dianhydride in NMP, and second, the polycondensation solution was treated by thermal imidization. The well-defined 'hard particles' (POSS) and the strong covalent bonds between the PI and the 'hard particles' lead to a significant improvement in the thermal mechanical properties of the resulting nanocomposites. The glass transition temperature dramatically increases while the coefficient of thermal expansion (CTE) decreases, owing to the significant increase of the cross-linking density in the PI–POSS nanocomposites. The thermal stability and mechanical property of the nanocomposites were also improved.
© 2003 Published by Elsevier Science Ltd.

Keywords: Nanocomposites; Polyimide; POSS

1. Introduction

Polyimides (PIs) are widely used in microelectronic industries because of their outstanding characteristics, such as excellent tensile strength and modulus, good thermal stability and dielectric property, and good resistance to organic solvents [1–6]. With the miniaturization of IC, applications such as circuit-printing films and semiconductor coatings however require the PIs to possess lower coefficient of thermal expansion (CTE), higher glass transition temperature and better thermal mechanical strength to avoid debonding between PIs and inorganic substrate and flaws in the PI interlayer. Incorporation of inorganic materials such as ceramics, silsesquioxane and silica nanoparticles has been proved very effective in providing enhancements in thermal mechanical property of PIs [7].

Organic–inorganic nanocomposite materials have been regarded as new generation of high performance materials since they combine the advantages of the inorganic materials (rigidity, high stability) and the organic polymers (flexibility, dielectric, ductility and processibility). Moreover, in comparison with macroscopic composites made of the same component phases they usually exhibit non-linear changes in optical, electrical, electro-optical and thermal mechanical properties [8–16]. One method of achieving organic–inorganic nanocomposites is to use the sol–gel process, which provides not only a chemical route to ceramics of high purity and controlled microstructure, but also can be coupled with polymeric materials processing to prepare organic–inorganic hybrid composites [17,18]. The process normally consists of two steps, the first step is the hydrolysis of a metal alkoxide, and the second step is the polycondensation of the resulting hydrolysis products. Alternately, clays that consist of 1 nm thick silicate sheets have been extensively used as reinforcement agents to develop polymer-layered silicate nanocomposites with improved physico-mechanical properties [19,20]. The efficiency of the clays to modify the properties of the polymer is primarily determined by the degree of its dispersion in the polymer matrix. As polymers are imbibed between the silicate sheets, the clays tend to exist as many exfoliated sheets in the clay/organic nanocomposites, as a result, the thermal mechanical properties of nanocomposites are enhanced significantly [21,22].

* Corresponding author. Tel.: +65-6874-8145; fax: +65-6872-7528.
E-mail address: cb-he@imre.a-star.edu.sg (C. He).

0032-3861/03/$ - see front matter © 2003 Published by Elsevier Science Ltd.
doi:10.1016/S0032-3861(03)00434-8

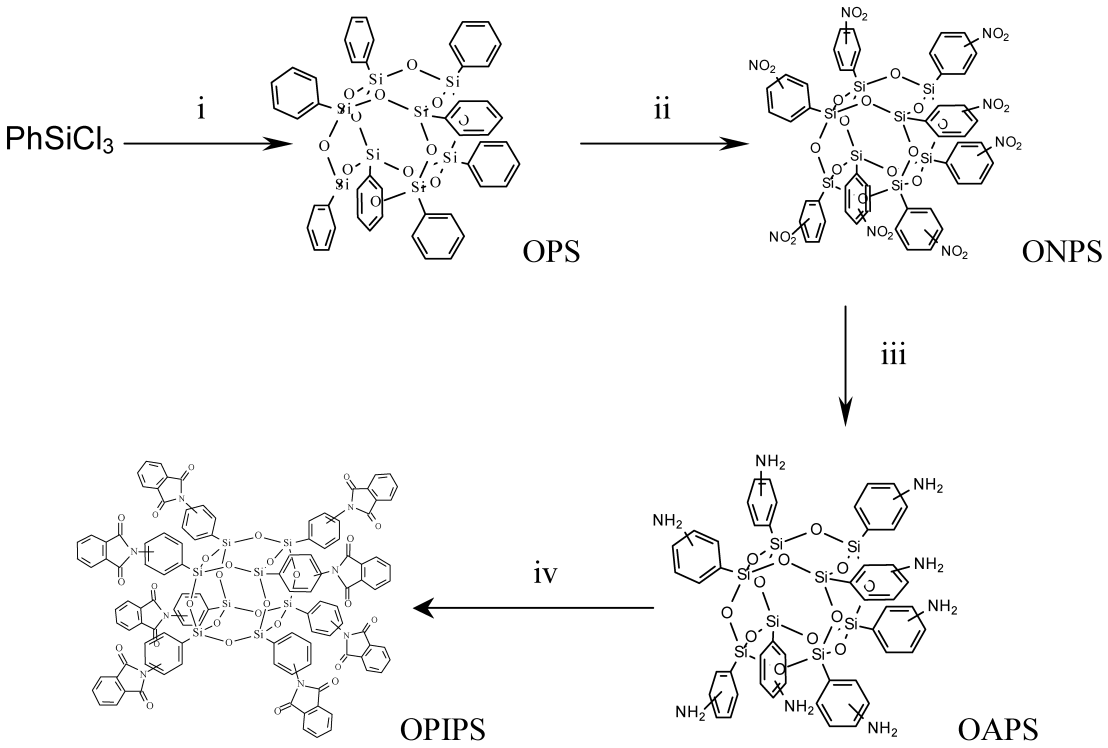

Scheme 1. (i) H_2O, benzene, benzyltrimethylammonium hydroxide, stir at RT/N_2. (ii) Fuming nitric acid, stir at RT. (iii) Pd/C, THF, NEt_3, HCO_2H, reflux, 60 °C. (iv) Phthalic anhydride, NMP, 270 °C.

Recently, a series of thermoset organic–inorganic hybrid composites based on several types of octa-functional POSS have been prepared and studied by Laine's group [23–26]. In these composites, the cubic silica cores are completely defined as 'hard particles' with a 0.53 nm diameter and a spherical radius of 1–3 nm including peripheral organic units. The size of cubic silsesquioxanes is at nanometer scale and mono-dispersed. If in a hybrid composite, these hard particles are linked to organic component with known architecture, a nanocomposite with completely defined interfacial component between organic and inorganic phase can be obtained. In this paper, we describe the formulation, preparation and properties of PI/POSS nanocomposites. The nanocomposites were prepared based on octa(aminophenyl)silsesquioxane (OAPS, Scheme 1) with a radius of 1.3 nm including rigid silica core and eight phenyl groups. We found that the thermal mechanical properties of PI–POSS nanocomposites were significantly improved in comparison with the pure PI.

2. Experimental

2.1. Materials

Phenyltrichlorosilane was purchased from Aldrich. 4,4′-diaminodiphenylmethane (MDA), 3,3′, 4, 4′-benzophenonetetracarboxylic dianhydride (BPTA) and fuming nitric acid were from Sino Chemical Co. Ltd Anhydrous grade *N*-methyl-2-pyrrolidinone (NMP) was purified by distillation under a nitrogen atmosphere and dried over molecular sieves. Tetrahydrofuran (THF) was distilled under nitrogen atmosphere from Na/benzophenone immediately prior to use. Triethylamine was distilled from CaH_2 under nitrogen atmosphere immediately prior to use. Other chemicals were used as purchased unless mentioned.

2.2. Instrumentation

FTIR spectra were recorded on a Perkin–Elmer SPECTRUM-2000 FTIR spectrophotometer with KBr pellets. ^{1}H NMR, ^{13}C NMR spectra were collected on a Bruker 400 spectrometer using Acetone-d_6 or chloroform-*d* as solvent and tetramethylsilane as internal standard. Solid-state ^{29}Si NMR spectra were also recorded on the Bruker 400 spectrometer with the frequency of 79.5 MHz. Dynamic mechanical analysis (DMA) measurements were performed using a TA Instruments DMA 2980, a heating rate of 5 °C/min and a frequency of 1 Hz were used. Thermomechanical analyses (TMA) were performed using a TA Instruments TMA 2940 at a heating rate of 5 °C/min. The thermal stability was characterized using a TGA 2050 thermogravimetric analyzer of TA Instruments at a heating rate of 20 °C/min. All the thermal analysis experiments were conducted in nitrogen atmosphere. The mechanical properties of the PI and the PI–POSS nanocomposites were tested on an Instron universal tester at a drawing rate of 5 mm/min.

2.3. Octaphenylsilsesquioxane

This was synthesized following literature [27]. Phenyltrichlorosilane (10.9 g, 0.05 mol) was dissolved in 50 ml of benzene and shaken with 100 ml water for 5 h. After removing the acid layer, the benzene layer was washed with water and added with 1.2 ml (3 mmol) of 40% benzyltrimethylammonium hydroxide/methanol solution. The mixture was refluxed for 4 h, then allowed to stand 4 days. The mixture was refluxed again for another 24 h, and then cooled and filtered to give white solid powder (6.1 g, 93%). FTIR (cm^{-1}): 3073, 1595, 1106; Solid ^{29}Si NMR (ppm): −65.2.

2.4. Octa(nitrophenyl)silsesquioxane

This was synthesized by following Laine's method [26]. 10 g of Octaphenylsilsesquioxane (OPS) (9.7 mmol) was added in small portions to 50 ml of fuming nitric acid with stirring at 0 °C. When the addition was completed, the solution was stirred at 0 °C for half an hour and then at room temperature for 20 h. After filtration through glass frit, the solution was poured onto 50 g of ice. A faintly yellow precipitate was collected by filtration and washed with water. The obtained powder was dried under vacuum at 40 °C; the yield is 88% (11.9 g). ^{1}H NMR (acetone-d_6, ppm): 8.7 (t, 1.0H), 8.5–8.0 (m, 4.8H), 7.8 (m, 3.5H); ^{13}C NMR (acetone-d_6, ppm) 153.2, 148.3, 140.9, 138.2, 135.5, 133.8, 132.6 (small), 130.8, 128.9, 126.8, 125.0; solid ^{29}Si NMR (ppm): −67.1 ($PhSiO_3$), −70.8 ($PhSiO_3$); FTIR (cm^{-1}): 1348 (N=O), 1530 (N=O), 1110 (Si–O–Si); GPC (THF): M_n 1168, M_w 1204, M_w/M_n 1.03.

2.5. Octa(aminophenyl)silsesquioxane

This was prepared by following Laine's procedure with slight modification [26]. Octa(nitrophenyl)silsesquioxane (ONPS) (5.0 g, 3.58 mmol, $-NO_2$ 28.7 mmol) and 5 wt% Pd/C (0.61 g, 0.287 mmol) were charged into a flask with a condenser under N_2. Anhydrous THF (40 ml) and triethylamine (40 ml, 0.287 mol) were then added. The mixture was heated to 60 °C, and 98% formic acid (4.4 ml, 0.115 mol) was added dropwise into the mixture. The solution separated into two layers. After 5 h, the THF layer was separated. Another 30 ml of THF was added to the above solution, the mixture was stirred and the THF layer was separated again. The combined THF extraction was filtered through Celite. The filtrate was added 40 ml of ethylacetate and washed with H_2O three times. The organic layer was dried by $MgSO_4$ and precipitated into 1 l of hexane. A white precipitate was collected by filtration. The white product was further purified by re-dissolved in mixture of 30:50 THF/ethyl acetate solvent and precipitated into 600 ml hexane. The obtained powder was dried under vacuum; the achieved Yield is 61% (2.5 g). ^{1}H NMR (acetone-d_6, ppm): 7.8–6.0 (b, 4.0H), 5.2–3.5 (b, 2.0H); ^{13}C NMR (acetone-d_6, ppm) 154.0, 148.5, 136.2, 132.5, 129.3, 123.7, 119.8, 116.8, 115.4; ^{29}Si Solid NMR (ppm): −63.1 ($PhSiO_3$), −66.7 (shoulder, $PhSiO_3$); FTIR (cm^{-1}): 3367 (NH_2), 1116 (Si–O–Si); GPC (THF): M_n 1058, M_w 1094, M_w/M_n 1.04.

Table 1
The preparation formulation of the PI–POSS nanocomposites

Entry	Amine group ratio[a]	Mole ratio[b]	OAPS[c] (wt%)	Remarks
PI	–	100:100:0	0.00	Transparent
a	1:20 (0.05)	105:100:0.625	2.70	Transparent
b	1:10 (0.1)	105:100:1.25	5.27	Transparent
c	2:10 (0.2)	105:100:2.5	10.02	Transparent
d	2:5 (0.4)	105:100:5	18.22	Transparent

[a] Amine group ratio is the ratio of the amine group number of OAPS vs. the amine group number of the diamine.
[b] Mole ratio is the mole ratio of BPTA, MDA and OAPS.
[c] The content of OAPS was theoretical value.

2.6. Preparation of PI–POSS nanocomposites

The PI–POSS nanocomposites were prepared by a conventional procedure depicted in Fig. 4 A three-neck flask was first purged with nitrogen gas to remove moisture. To the above flask, a MDA (10 mmol, 1.98 g)/NMP (40 ml)

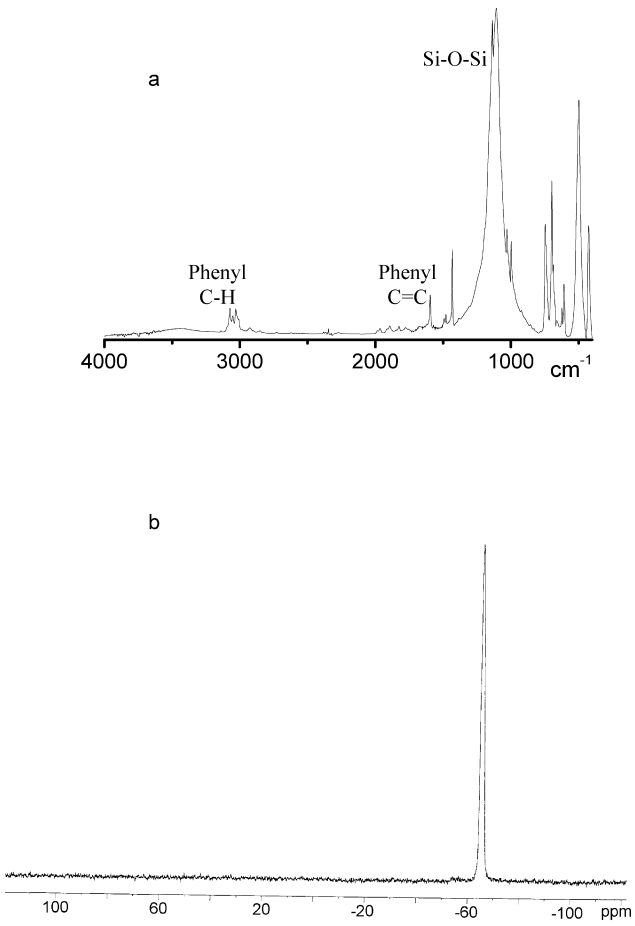

Fig. 1. FTIR spectrum (a) and Solid ^{29}Si NMR spectrum (b) of OPS.

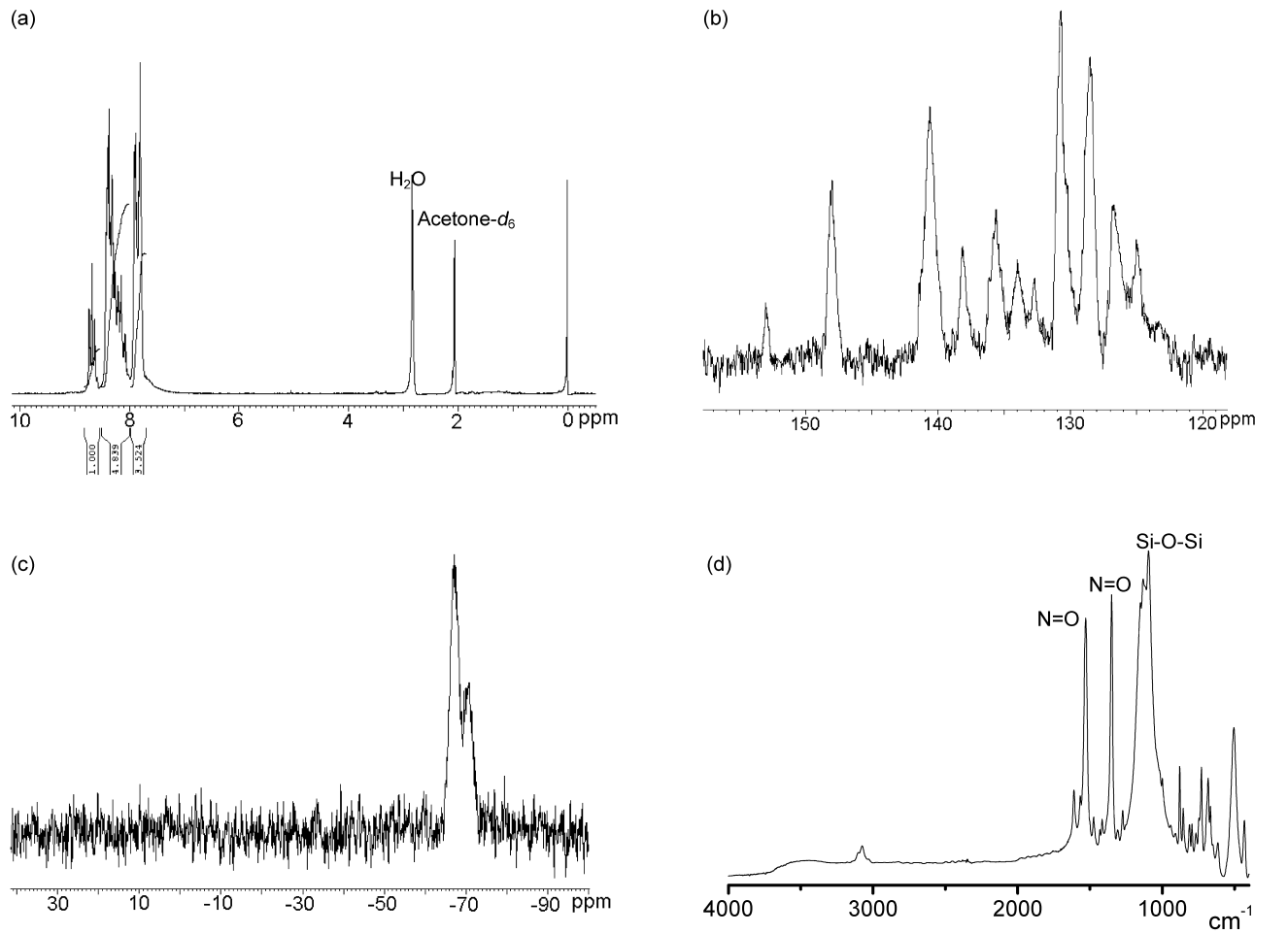

Fig. 2. ^{1}H NMR spectrum (a), ^{13}C NMR spectrum (b), solid ^{29}Si NMR spectrum (c) and FTIR spectrum (d) of ONPS.

solution was added and followed by BPTA (10.5 mmol, 3.38 g) in five portions. The mixture was stirred under N_2 at room temperature for 6 h, and a viscous polyamic acid (PAA) solution was obtained. To this PAA solution, a predetermined amount of OAPS/NMP solution was added. The mixture was stirred at room temperature for additional 2 h to give a transparent solution. The solution was then cast on a glass substrate and thermally treated at 80 °C for 12 h, 120 °C for 4 h, 200 °C for 2 h, and 270 °C for 2 h. The films were removed from the glass substrates with the aid of deionized water and dried at 100 °C in a vacuum oven; the thickness of the films was about 50 um. The compositions of the PI–POSS nanocomposites samples are listed in Table 1.

3. Results and discussion

3.1. Structure of POSS

OAPS was synthesized according to Laine's method with a slight modification [26]. OAPS was prepared in a two-step reaction, i.e. nitration of OPS to form ONPS, and then followed by hydrogen-transfer reduction to yield OAPS (Scheme 1). FTIR, ^{1}H, ^{13}C and ^{29}Si NMR spectra of OPS, ONPS and OAPS were shown in Figs. 1–3, respectively. Formation of *meta* isomer and *para* isomer and cage retention of OAPS were supported by these data. The FTIR spectra and the ^{1}H NMR spectra of ONPS and OAPS indicated a complete conversion of nitric groups into amine groups. In the ^{1}H NMR spectrum of OAPS the aromatic peaks of ONPS disappear completely and new aromatic peaks appear at higher magnetic field. Likewise, in the FTIR spectrum of OAPS, the peaks at 1348 and 1530 cm^{-1} (νN=O) disappear while new broad peak at 3367 cm^{-1} (νN–H) is observed. In Figs. 2(c) and 3(c), two peaks (−67.1 ppm, −70.8 ppm) were observed in solid ^{29}Si NMR spectrum of ONPS, the peaks at −63.1 ppm and at −66.7 ppm (shoulder) were also shown in the ^{29}Si NMR spectrum of OAPS, suggesting that two isomers are formed. Ten primary peaks correspond to ten different carbon environments of both isomers were observed in the ^{13}C NMR spectrum of ONPS (Fig. 2(b)) with one small peak [26], and ten peaks were also observed in ^{13}C NMR spectrum of OAPS (Fig. 3(b)). For the ^{1}H NMR spectrum of ONPS no speak at about 9 ppm was observed. In the ^{1}H NMR spectrum of OAPS, the integration ratio of peaks

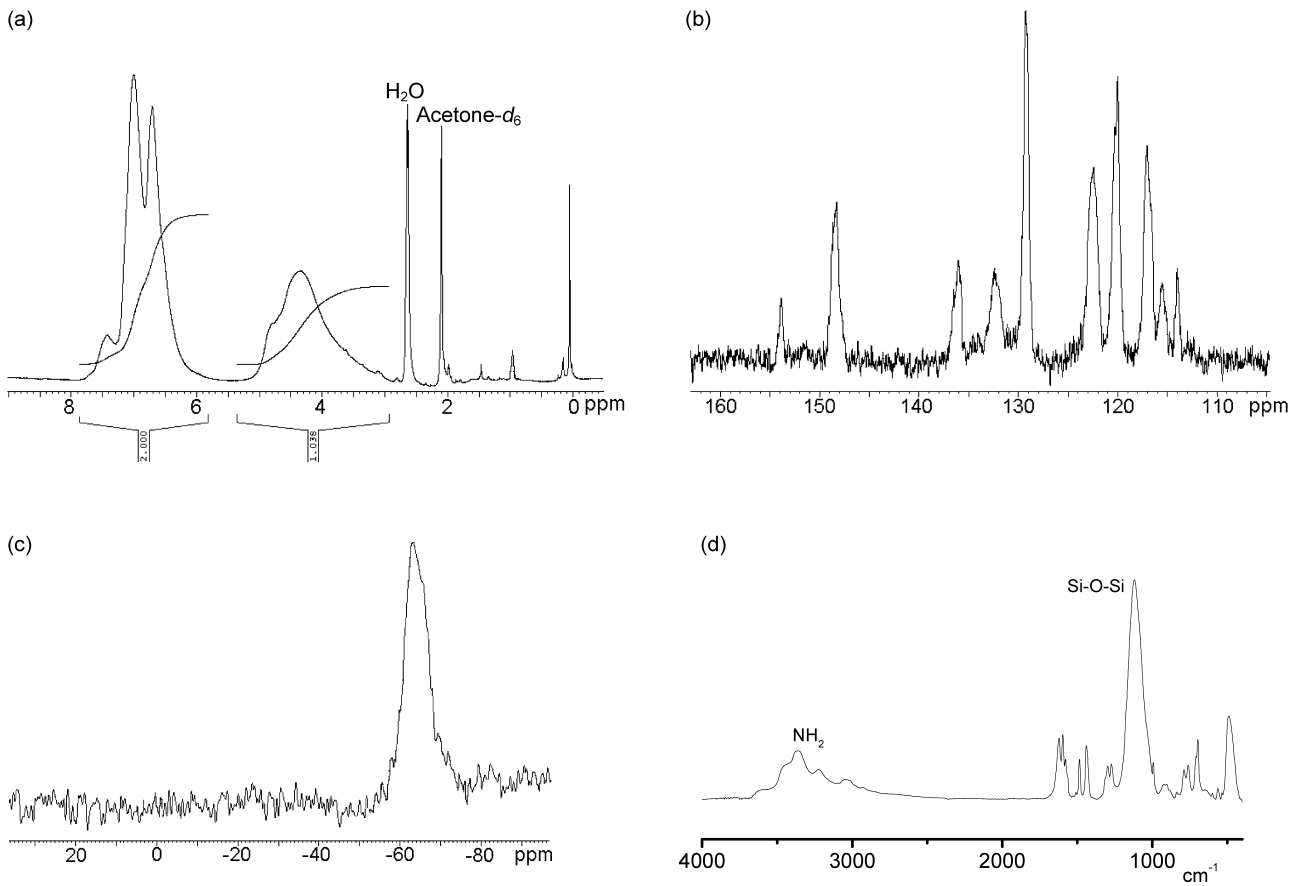

Fig. 3. ^{1}H NMR spectrum (a), ^{13}C NMR spectrum (b), solid ^{29}Si NMR spectrum (c) and FTIR spectrum (d) of OAPS.

correspond to the amine groups and the aromatic groups equals to 1:2. These results indicate that both isomers have eight nitro groups or amine groups. The triplet peaks at 8.7 ppm were assigned to protons between the nitro group and the siloxy group in the *meta* isomer [26]. The percent of *meta* isomer and *para* isomer can be estimated as 48.2 and 51.8%, respectively. The cage structures of OPS, OAPS and ONPS were confirmed by solid ^{29}Si NMR spectra, because no peak exists in all ^{29}Si NMR spectra, except the peaks of the cubic silicon. The narrow polydispersity of ONPS and OAPS provided by GPC data also confirm retention of the cage structure.

3.2. PI–POSS nanocomposites

The PI and the PI–POSS nanocomposites were normally prepared by reaction of diamine and carboxylic dianhydride in a two-step method (Fig. 4). Fig. 5 shows the FTIR spectra of each step of imidization procedure. The absorption bands at 1778 cm^{-1} (unsymmetric νC=O in imide groups),

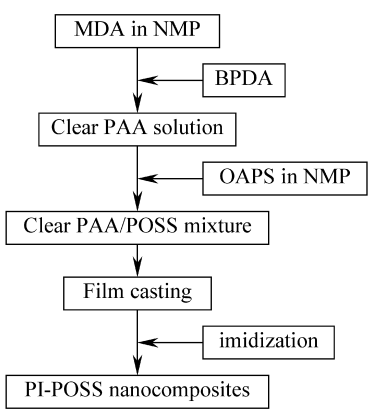

Fig. 4. Preparation flow diagram of the PI–POSS nanocomposites.

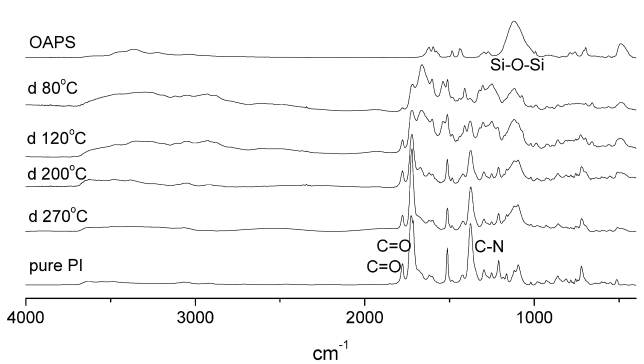

Fig. 5. FTIR spectra of OAPS, PI–POSS nanocomposite and PI. The mole ratio of BPTA, MDA and OAPS in sample d is 105:100:5.

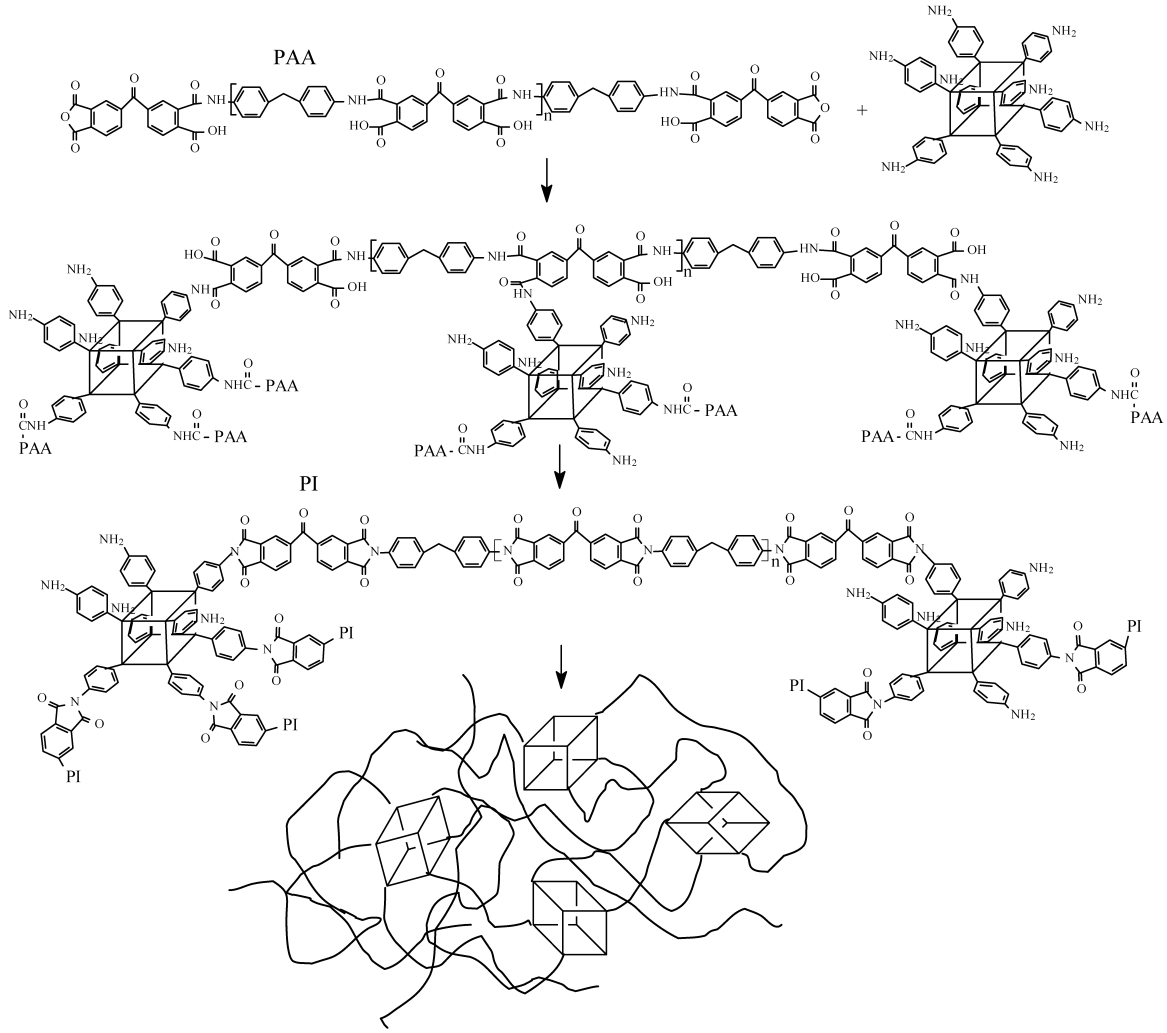

Scheme 2. Schematic representation of linkage between the PI chains and the OAPS cages.

1727 cm^{-1} (symmetric νC=O in imide groups) and 1378 cm^{-1} (νC–N in imide groups) [2,28] increased with increase in imidization temperature. The absorption bands of the amide groups at ~1660 cm^{-1} (νC=O) and ~1550 cm^{-1} (νC–N) are absent when the imidization temperature increases to 270 °C, indicating that the amide bonds completely disappear. The absorption band of POSS at 1120 cm^{-1} (asymmetric νSi–O–Si) was observed in the all spectra of the PI–POSS nanocomposites.

OAPS is 'organic–inorganic hard particles' consist of the cubic silica core and eight amino-phenyl groups. It can be easily dissolved in NMP that facilitates a proper mixing between POSS and PAA in NMP solvent. The PAA in this study was terminated by anhydride groups, since a small excess amount (5% mole) of the dianhydride was added. Scheme 2 shows the tether structure between OAPS and PI during the imidization process. When the OAPS/NMP solution was mixed with the PAA/NMP solution, the amine groups of OAPS will react with the terminal anhydride groups of PAA, which results in the formation of amide bonds between POSS and PAA. During the imidization process, the amide bonds are converted into imide groups. As a result, the linkage between the PI and the POSS is the phenyl group and the imide group.

Alternately, the amine groups of OAPS may react with the side carboxylic groups of the PAA to form amide bonds. However, the chance of forming the amide bonds between POSS and side carboxyl groups is small due to the low reactivity of the side carboxyl groups. Furthermore, this kind of the ortho amide bonds aren't stable in the process of imidization. Two adjacent amide bonds are transformed into one amine group and one imide group [29]. But linkage between the PI and the POSS is still the phenyl group and the imide group (Scheme 2). This tether structure has been verified by FTIR spectra of the PI–POSS nanocomposites (Fig. 5).

In order to further confirm the tether structure in the PI–POSS nanocomposites and the effects of curing temperature on the thermal stability of the POSS core, we use octa(phthalimidephenyl)silsesquioxane (OPIPS) as model compound because its structure is similar to the tether structure of PI–POSS nanocomposites [26,30]. OAPS and

phthalic anhydride were mixed in NMP at room temperature and stirred for 1/2 h; the mixture was heated at 80 °C for 12 h, 120 °C for 4 h, 200 °C for 2 h, 270 °C for 2 h, respectively. The characterization results are shown in Fig. 6. ^{1}H NMR spectrum shows a new broad aromatic peak (6.7–8.1 ppm) and the amino peaks of OAPS disappear completely. Likewise, ^{13}C NMR spectrum shows new aromatic peaks at 134.1, 132.3, 131.4, 128.7, 123.5 ppm and a new carbonyl peak at 167.2 ppm. No original peaks of OAPS was observed in ^{13}C NMR spectrum. Symmetric and asymmetric νC=O (in imide groups) bands at 1777 cm^{-1} and 1721 cm^{-1} and a νC–N (in imide groups) band at 1377 cm^{-1} are observed in FTIR spectrum, respectively. The molecular weights of OPIPS obtained from GPC (THF) are M_n (1793) and M_w (1923), which are increased comparing with those of OAPS. The polydispersity of OPIPS (M_w/M_n 1.07) remains narrow, indicating the intact cage structure of OPIPS. All the results confirm the formation of the octaphthalimide structure.

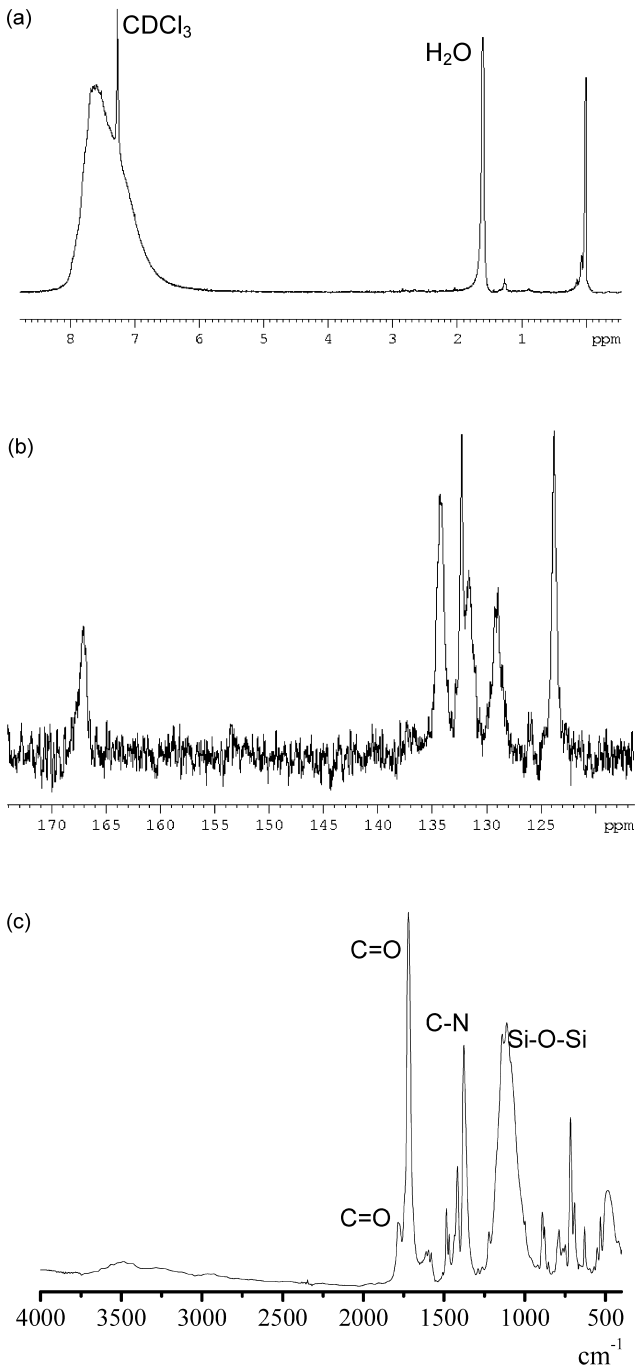

Fig. 6. ^{1}H NMR spectrum (a), ^{13}C NMR spectrum (b) and FTIR spectrum (c) of OPIPS.

The dynamic mechanic analyses (DMA) performed on the pure PI films and the PI–POSS nanocomposites films of various amine group ratios are shown in Fig. 7. As the amine group ratios increase, the tan δ peaks of each PI–POSS nanocomposites shift significantly to a higher temperature while the widths of tan δ peaks remarkably broaden, and their intensities lower. The PI–POSS nanocomposites exhibit a significant higher T_g than that of the pure PI. T_g increases from 301.4 °C for the pure PI to 421.0 °C for the PI–POSS nanocomposite of the amine group ratio 0.4 (about 120 °C increase). The storage moduli of the PI–POSS nanocomposites below and above its T_g increase with the increase of OAPS concentration. The increase of glass transition temperature with incorporation of POSS could be two-fold. First, incorporation of POSS increases the cross-linking density of the resulting nanocomposites. Second, POSS is a rigid body; increase of POSS concentration would increase the rigidity of the composite system. The increase in cross-linking density leads to high T_g, broad tan δ peak and high storage modulus [31]. Although, incorporation of POSS increases the free volume in the PI–POSS nanocomposites, this effect can be compensated by the increase in the cross-linking density.

Table 2 and Fig. 8 show the thermal properties of the pure PI and the PI–POSS nanocomposites. The thermal stabilities of the PI–POSS nanocomposites increase as the

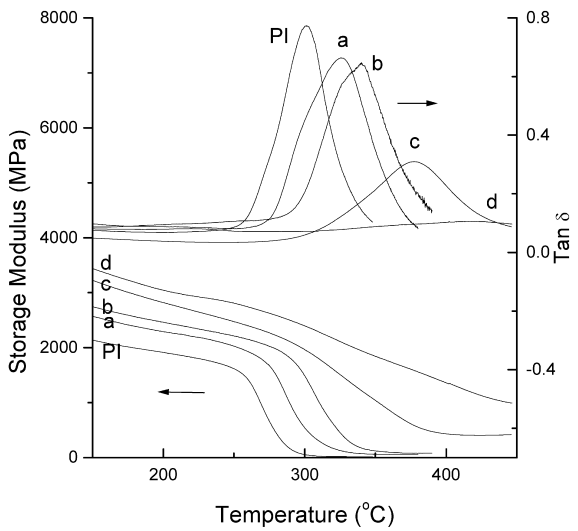

Fig. 7. DMA curves of the PI–POSS nanocomposites and the pure PI. The mole ratios of BPTA, MDA and OAPS in sample a, b, c and d are 105:100:0.625, 105:100:1.25, 105:100:2.5 and 105:100:5, respectively.

Table 2
Thermal properties of the PI–POSS nanocomposites and the pure PI

Entry	PI	a[a]	b[a]	C[a]	d[a]
T_g (DMA, °C)	301.4	326.3	340.1	377.4	421.0
T_d (onset,° C)[b]	524.7	529.5	531.1	533.1	536.5
T_d (5%,°C)[c]	513.5	524.8	537.6	550.4	551.2

[a] The mole ratios of BPTA, MDA and OAPS in sample a, b, c and d are 105:100:0.625, 105:100:1.25, 105:100:2.5 and 105:100:5, respectively.
[b] Thermal decomposition temperature of onset point.
[c] Thermal decomposition temperature of 5% mass loss.

amine group ratios increase from 0 to 0.4. The decomposition temperatures determined by TGA (on-set temperature and 5% mass loss temperature) increase from 524.7, 513.5 °C for the pure PI to 536.5, 551.2 °C for the PI–POSS nanocomposites of the amine group ratio 0.4. The cubic silica cores and the phenyl groups with good thermal stability and the stable covalent bonds between two components limit the continuous decomposition of the PI phase. The mass retained around 800 °C is proportional to the OAPS content in the PI–POSS nanocomposites.

The coefficients of thermal expansion of the PI–POSS nanocomposites are shown in Fig. 9. The CTEs of the PI–POSS nanocomposites decrease dramatically with increase in the content of OAPS. The CTEs of the pure PI and the PI–POSS nanocomposites of 0.1 amine group ratio are 65.8 and 46.6 ppm/K, respectively. When the amine group ratio increases to 0.4, the CTE of the PI–POSS nanocomposite decreases to 37.4 ppm/K, which is less than 60% of the CTE of pure PI. The decrease in CTE could be attributed to the increase in cross-linking density and the low CTE of rigid POSS [32]. It is also observed that the reduction of CTE is significant at low content of POSS. With an increase of POSS content, the CTE decreases slowly and then level off.

The effects of OAPS content on the mechanical properties of the PI–POSS nanocomposites are shown in Fig. 10

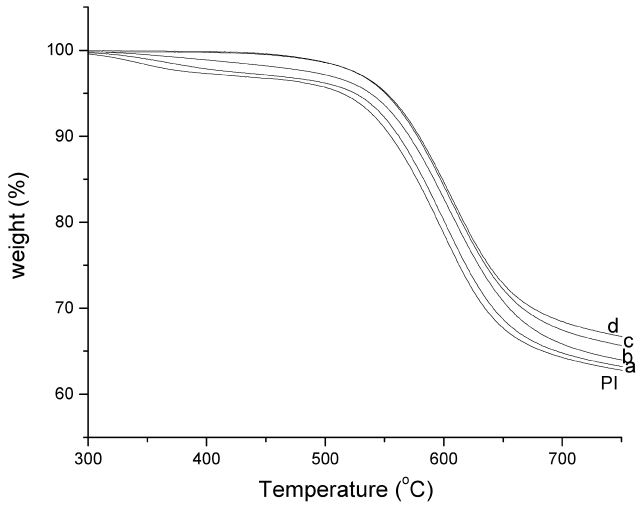

Fig. 8. TGA curves of the PI–POSS nanocomposites and the pure PI. The mole ratios of BPTA, MDA and OAPS in sample a, b, c and d are 105:100:0.625, 105:100:1.25, 105:100:2.5 and 105:100:5, respectively.

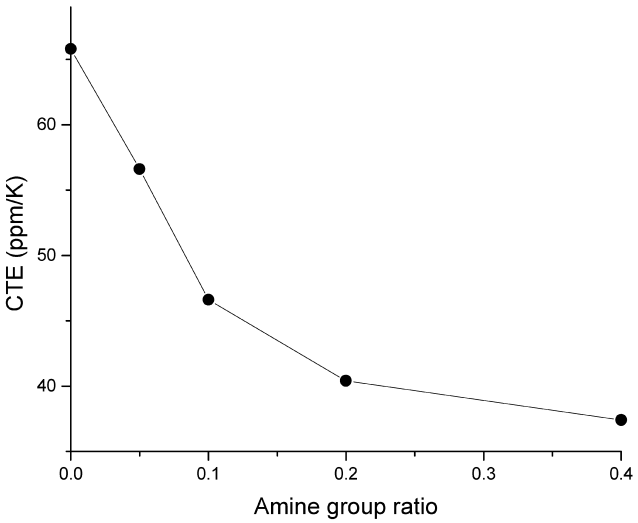

Fig. 9. The coefficients of thermal expansion (CTE) of the PI–POSS nanocomposites vs amine group ratio. Amine group ratio is the ratio of the amine group number of OAPS vs. the amine group number of the diamine.

and Table 3. Fig. 8 shows the relationship between the amine group ratios and the initial moduli and storage moduli of the PI–POSS nanocomposites. The introduction of the OAPS, which has a higher modulus than the PI matrix, leads to an increase in the moduli of the PI–POSS nanocomposites. For the amine group ratio less than 0.2, the initial moduli increase almost linearly proportion to the increase of the amine group ratio, suggesting the cross-linking density in PI–POSS nanocomposites may be proportional to the amine group ratio when it is less than 0.2. As the amine group ratio is further increased, the cross-linking density in the PI–POSS nanocomposites tends to level off, so do the moduli of the PI–POSS nanocomposites.

The tensile strength and the elongation at break of the pure PI and the PI–POSS nanocomposites are listed in

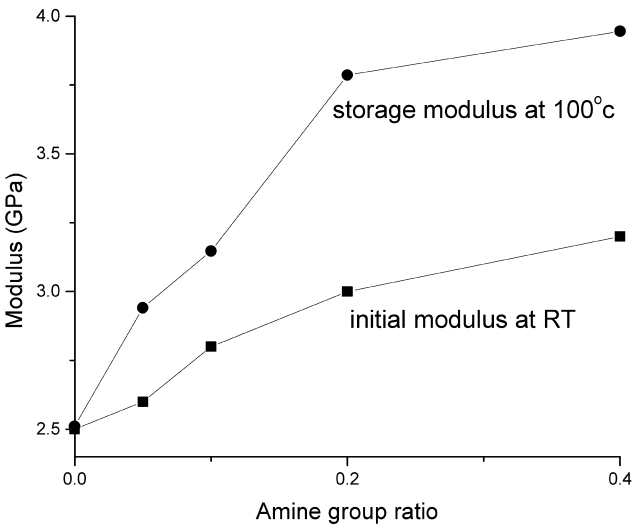

Fig. 10. Moduli of the PI–POSS nanocomposites vs amine group ratio. Amine group ratio is the ratio of the amine group number of OAPS vs. the amine group number of the diamine.

Table 3
The mechanical properties of the PI–POSS nanocomposites and the pure PI

Entry	PI	a[a]	b[a]	c[a]	d[a]
Initial modulus (GPa)	2.5	2.6	2.8	3.0	3.2
Tensile strength (MPa)	82.2	98.9	90.1	61.7	42.4
Elongation at break (%)	7.5	8.0	7.1	3.9	2.0

[a] The mole ratios of BPTA, MDA and OAPS in sample a, b, c and d are 105:100:0.625, 105:100:1.25, 105:100:2.5 and 105:100:5, respectively.

Table 3. When the amine group ratio is 0.05, both the tensile strength and the elongation at break increase from 82.2 MPa, 7.5% to 98.9 MPa, 8.0%, respectively. The PI is strengthened and toughened simultaneously. When the amine group ratio exceeds 0.1, both the tensile strength and the elongation at break decrease, possibly due to high cross-linking density in the PI–POSS nanocomposites.

4. Conclusions

Novel PI–POSS nanocomposites with precisely defined nano-scale inorganic phase were successfully prepared using a conventional approach. The resulting PI–POSS nanocomposites exhibit excellent thermal mechanical properties, such as high glass transition temperature and low CTE. For example, significant increase in glass transition temperature (from 301.4 °C for pure PI to 421.0 °C for PI–POSS nanocomposite at an amine group ratio 0.4) and dramatic decrease in CTE, improved thermal stability and increase in modulus. The mechanical properties of nanocomposites can be strengthened and toughened at the same time by incorporation of the proper amount of OAPS.

Acknowledgements

We are grateful to Prof. Laine and Dr Kim S. for valuable advice and demo synthesis of OAPS. This research was supported by DSO national lab of Singapore and Institute of Materials Research and Engineering, Singapore.

References

[1] Feit C, Wilkins Jr.C. Polymer materials for electronic applications. ACS symposium series 184, Washington, DC: American Chemical Society; 1982.
[2] Feger G, Khojasteh MM, McGrath JE, Polyimides: materials, chemistry and characterization, Amsterdam: Elsevier; 1989.
[3] Gosh MK, Mittal KL. Polyimides: fundamentals and applications. New York: Marcel Dekker; 1996.
[4] Mittal KL. Polyimides. New York: Plenum Press; 1984.
[5] Saroog CJ. Polym Sci Macromol Rev 1976;11:161.
[6] Numata S, Kinjo N. Polym Engng Sci 1988;28:906.
[7] Ahmad Z, Mark JE. Chem Mater 2001;13:3320.
[8] Lan T, Pinnavaia TJ. Chem Mater 1994;6:2216.
[9] Huang JC, Zhu ZK, Ma XD, Qian XF, Yin J. J Mater Sci 2001;36:871.
[10] Huang JC, Zhu ZK, Yin J, Qian XF, Sun YY. Polymer 2001;43:873.
[11] Messersmith PB, Giannelis EP. J Polym Sci, Part A: Polym Chem 1995;33:1047.
[12] Burnide SD, Giannelis EP. Chem Mater 1995;7:1597.
[13] Huang XY, Heulings HR, Le V, Le J. Chem Mater 2001;13:3754.
[14] Meldrum A, Haglund RF, Boatner LA, White CW. Adv Mater 2001; 13:1431.
[15] Ye JY, Balogh L, Norris TB. Appl Phys Lett 2002;80:1713.
[16] De Sande JCG, Serna R, Gonzalo J, Afonso CN, Hole DE, Naudon A. J Appl Phys 2002;91:1536.
[17] Mark JE, Lee CY-C, Bianconi PA. Hybrid organic–inorganic composites. Washington, DC: American Chemical Society; 1995.
[18] Chujo Y. Curr Opin Solid State Mater Sci 1996;1:806.
[19] Ogawa M, Kuroda K. Chem Rev 1995;95:399.
[20] Pinnavaia TJ. Science 1983;220:365.
[21] Mark JE. Polym Sci Engng 1996;36:2905.
[22] Giannelis EP. Adv Mater 1996;8:29.
[23] Choi J, Harcup J, Yee AF, Zhu Q, Laine RM. J Am Chem Soc 2001; 123:11420.
[24] Zhang C, Babonneau F, Bonhomme C, Laine RM, Soles CL, Hristov H, Yee AF. J Am Chem Soc 1998;120:8380.
[25] Zhang C, Laine RM. J Am Chem Soc 2000;122:6979.
[26] Tanaki R, Tanaka Y, Asuncion MZ, Choi J, Laine RM. J Am Chem Soc 2002;123:12416.
[27] Brown Jr. JF, Vogt Jr. LH, Prescott PI. J Am Chem Soc 1964;86:1120.
[28] Mittal KL. Polyimides: synthesis, characterization and applications. New York: Plenum Press; 1984.
[29] Dine-Hart RA, Wright WW. J Appl Polym Sci 1967;11:609.
[30] Tamaki R, Choi J, Laine RM. Chem Mater 2003;15:793.
[31] Tsai MH, Whang WT. J Appl Polym Sci 2001;81:2500.
[32] Huang JC, Zhu ZK, Yin J, Zhang DM, Qian XF. J Appl Polym Sci 2001;79:794.